

To Appear in the Astronomical Journal (April 2004)

Eta Carinae's Brightness Variations Since 1998: HST Observations of the Central Star^{2,3}

J. C. Martin

`martin@aps.umn.edu`

*University of Minnesota Astronomy Department
Minneapolis, MN 55455*

M. D. Koppelman

`michael@aps.umn.edu`

*University of Minnesota Astronomy Department
Minneapolis, MN 55455*

and

the HST Eta Carinae Treasury Project Team¹

ABSTRACT

We have measured the brightness variations in η Carinae for the past six years using the Hubble Space Telescope Space Telescope Imaging Spectrograph and Advanced Camera for Surveys. Unlike ground-based data, observations by the HST allow direct measurement of the brightness of the central star by resolving it from the surrounding bright ejecta. We find interesting behavior during

¹This research was conducted as part of the Eta Carinae Hubble Space Telescope Treasury project via grant no. GO-9420 from the Space Telescope Science Institute. The HST is operated by the Association of Universities for Research in Astronomy, Inc., under NASA contract NAS5-26555.

²Some of the data presented in this paper were obtained from the Multi-mission Archive at the Space Telescope Science Institute (MAST). STScI is operated by the Association of Universities for Research in Astronomy, Inc., under NASA contract NAS5-26555. Support for MAST for non-HST data is provided by the NASA Office of Space Science via grant NAG5-7584 and by other grants and contracts.

³Some of the data presented in this paper were obtained from the American Association of Variable Star Observers International Database.

2003 in the continuum and $H\alpha$ emission. The data show that the established long term brightening trend of η Car continues, including regular events which coincide with the 5.5 year spectroscopic cycle and other more rapid and unexpected variations. In addition to the HST data, we also present ground-based data obtained from the AAVSO which show many of the same features. The dip in the apparent brightness of the central star at the time of the 2003.5 event is wavelength dependent with no decrease in the continuum. These observations cast doubt on a simple eclipse or occultation as the explanation for the dip and place constraints on the models for the event.

Subject headings: STARS: ACTIVITY, STARS: INDIVIDUAL: CONSTELLATION NAME: ETA; CARINAE, STARS: PECULIAR

1. Introduction

Two unforeseen developments in recent years have made continued photometry of η Car particularly important: Distinctive brightness variations in the near IR accompany its mysterious 5.5-year spectroscopic cycle (Feast, Whitelock, & Marang 2001; Whitelock et al. 1994) and, possibly independent of the cycle (Damineli 1996), the star brightened at a surprising rate after 1997 (Davidson et al. 1999a,b; van Genderen, Sterken, de Groot, & Burki 1999; Sterken, Freyhammer, Arentoft, & van Genderen 1999). Neither of these phenomena has been explained and the data since 1998 are seriously incomplete. Meanwhile, the long-term brightening trend continues; for general information about η Car with many references, see Davidson & Humphreys (1997), and Davidson (2000).

Photometry of this bright object is difficult for at least two reasons:

1. At visual wavelengths, normal ground-based observations represent mainly the surrounding “Homunculus” ejecta-nebula, which appears much brighter than the central star and has structure at all radii from 0.2 to 8 arcseconds. So far the only available measurements of just the central star have been made with the Hubble Space Telescope (HST). Although the Homunculus is primarily a reflection nebula, its apparent brightness measured with respect to the central star has changed greatly. During 1998-99, while ground-based observations showed about a 0.3-magnitude brightening of Homunculus plus star, the star itself nearly tripled in apparent brightness (Davidson et al. 1999b)! This discrepancy presumably involves dust along our line of sight to the star, but, as mentioned above, it is only vaguely understood at this time.

2. Numerous strong emission lines produced in the stellar wind perturb the results for standard photometric systems. $H\alpha$ and $H\beta$ emission, for example, have equivalent widths of about 800 and 180 Å respectively in HST spectra of η Car. Therefore, broad-band U , B , R , and I magnitudes, and most medium-band systems as well, are poorly defined for this object. Photometry around 5500 Å, e.g. broad-band V , is relatively free of strong emission lines, but transformations from instrumental magnitudes to a standard system are imprecise because they involve the other filters (Davidson et al. (1999b), Sterken, Freyhammer, Arentoft, & van Genderen (2001), van Genderen, Sterken, & Allen (2003a), and references therein).

In this paper we report photometry *of the central star* obtained with two HST instruments since 1998. For reasons noted above, these observations are quite distinct from all ground-based data; and the star’s photometric behavior during 2003 proved to be especially interesting. First we employ acquisition images produced by the Space Telescope Imaging Spectrograph (STIS), because these are numerous and internally reliable; η Car has been observed many times with this instrument since 1998, especially during mid-2003 when the most recent “spectroscopic event” occurred. These broad-band red data cannot be transformed to any standard photometric system, but they are quite reliable for showing relative fluctuations by the star (strictly speaking, the stellar wind), uncontaminated by light from the surrounding Homunculus. We also report surprising variations in the star’s $H\alpha$ emission brightness accompanied by measurements of the nearby continuum in the STIS slit-spectroscopy data.

We supplement the STIS data with similar measurements of a few images obtained in 2002–03 with HST’s Advanced Camera for Surveys (ACS). These represent a different set of wavelength bands. Altogether these STIS and ACS results probably represent most of the photometry of η Car that will ever be obtained with the HST. Very few additional STIS observations are expected now that the 2003 event has passed. Earlier HST/FOS, FOC, WFC-PC, and WFPC2 data were not obtained often enough to be suitable for our purposes, and in most cases would be more difficult to compare photometrically, for technical reasons. We report the STIS and ACS data now, rather than waiting for two or three more data points in 2004, because the behavior during 2003 was rather unexpected and therefore deserves to be noted promptly.

In addition, we briefly present a convenient summary of η Car’s photometric record in the AAVSO archives. These ‘V’ magnitudes represent, of course, the entire Homunculus plus star but they are valuable for comparisons with the HST data and also with ground-based photometry using different filter systems, reported by, e.g., Feast, Whitelock, & Marang (2001), van Genderen, Sterken, de Groot, & Burki (1999), Sterken, de Groot, & van Genderen

(1996), Whitelock et al. (1994), Fernandez Lajus et al. (2003), and van Genderen, Sterken, Allen, & Liller (2003b).

In Section 2 we present the photometry of the central star based on HST/STIS acquisition images and the ACS/HRC observations. This is followed by a section on the ground-based data from the AAVSO and then a general discussion about how these results relate to the models which have been presented to describe η Carinae.

2. Space-based Photometry of the Central Star

Normal ground-based imaging and photometry cannot resolve the central star and small structures in the Homunculus nebula. In this study, we have used the HST/STIS acquisition images which have a resolution of about 0.1 arcseconds plus the recent ACS/HRC images which have a resolution of 0.05 arcseconds to separate the contribution of central star from the surrounding nebulosity.

2.1. HST STIS Acquisition Images

Each set of STIS observations of η Carinae has included a pair of acquisition images. These images are 100x100 pixel sub-frames (5 arcseconds square) centered on the middle row and column of the CCD (Clampin et al. 1996; Downes et al. 1997; Kim Quijano et al. 2003). Each pair of acquisition images includes an initial targeting image and a post-acquisition image. Only the post-acquisition images were used to measure the brightness of the central star because the target is rarely well centered in the initial targeting images, which raises concerns about ghost images and internal reflections that may unpredictably affect them (see section 2.1.2).

The majority of the STIS acquisition images of η Carinae have been taken using the F25ND3 filter, which is a neutral density filter that covers the wavelengths from 2000Å to 11000Å. Acquisition images using other filters are ignored since they lack significant temporal baseline or coverage and there is little hope of transforming between filter functions for an object as peculiar as η Carinae. The F25ND3 filter includes several prominent features in the spectrum of η Carinae (Figure 1) and changes in them contribute to any measured brightness variations.

2.1.1. Image Processing and Bias Level Correction

We processed the STIS acquisition images using the IRAF¹ procedure `stas.hst.calib.stis.basic2d` with version 3.0 of STDAS and version 2.13 of CALSTIS. En lieu of a bias over-scan region, each STIS acquisition image has the uniform value of 1510 counts subtracted from each pixel as an approximate bias level correction for the target acquisition process. A small uncorrected bias level remains in the acquisition images after this initial correction, so we compensate for this tiny effect by modeling it as a function of time and CCD housing temperature.

This residual bias was measured in acquisition images of the standard star AGK +81 266 after the normal bias correction and dark current were subtracted. The exposures of AGK +81 266 are short (2.1 seconds) and it is more than 60 degrees above the ecliptic, so zodiacal light and other sources make a negligible contribution to the background (Kim Quijano et al. 2003). We found that the residual bias level in the images of AGK +81 266 (Figure 2) is roughly linear with respect to time prior to the failure of the CCD Side-1 controller on May 16, 2001 (Proffitt et al. 2002; Davis et al. 2001). There may be higher order terms in this relation however they are not significant in this study since they effect the measurements of the central star by less than 0.001 magnitude. Subsequent to the failure of the Side-1 controller the STIS CCD temperature regulator has been held at a constant voltage permitting the CCD temperature to fluctuate. As a result, after the Side-1 failure the residual bias level of the observations depends on both time and CCD housing temperature. Using the measurements of the residual bias level in the AGK +81 266 observations, the following relations were obtained for the bias level correction as a function of modified Julian Date (MJD) and CCD housing temperature (T):

MJD \leq 52045.5 :

$$BLEV = -269.84 - 0.0053 * MJD \quad (1)$$

MJD $>$ 52045.5 :

$$BLEV = -293.34 - 0.0053 * MJD - 1.51 * T \quad (2)$$

When the modeled bias level is subtracted from the AGK +81 266 data the background levels average to -0.03 ± 0.63 counts/pixel/sec (Figure 2). This correction was applied to the acquisition images for η Carinae in place of the bias over-scan correction normally implemented in the IRAF basic2d procedure. Typically the bias correction amounts to less than 0.005 magnitude for the measurements reported below.

¹IRAF is distributed by the National Optical Astronomy Observatories, which are operated by the Association of Universities for Research in Astronomy, Inc., under cooperative agreement with the National Science Foundation.

2.1.2. Aperture Photometry

The flux from the central star was measured in each image by summing detector counts within a small circular virtual aperture. In order to avoid pixelization effects, the counts were weighted by a function of the distance of a pixel from the aperture center (r) which decreases smoothly to zero at the aperture radius R :

$$r \leq R : f(r) = 1 - \frac{r^2}{R^2} \quad (3)$$

$$r > R : f(r) = 0 \quad (4)$$

The centering on the star is determined by a peak-up algorithm which locates the position where the sum inside the virtual aperture is maximized. For the STIS acquisition images we used $R = 3$ pixels which corresponds to a diameter of 0.3 arcseconds and includes slightly fewer than 30 pixels.

We did not attempt to subtract a background from the measured aperture flux, but this has little effect on the results since the star provides thousands of counts/pixel/second, far greater than any other contribution within the measuring aperture due to scattered and zodiacal light which contribute only about 0.2 counts/pixel/second or less (Kim Quijano et al. 2003). There is no feasible way to account for or remove the contribution from diffuse circumstellar material within 0.1 arcseconds of the star. However, STIS spectroscopic data indicate the level of contamination from this source is much smaller than the other uncertainties.

Ghost images exist in the STIS optics but do not contribute significantly to our measurements. When a bright source is centered on the CCD, a ghost image with an peak flux of a few percent relative to the PSF maximum appears approximately 0.3 arcseconds (6 pixels) to the right (increasing column number) of the peak of the point spread function. The 0.3 arcsecond diameter aperture used to measure the central star excludes this ghost. However, any future work that may attempt to measure the flux from the nebula immediately surrounding the central star in these images must confront this problem.

The reduction procedure was tested using 80 pairs of acquisition images of the flux standard AGK +81 266 (Figure 3). The measured aperture photometry for this standard shows a constant level with an r.m.s scatter of ± 0.037 magnitudes. It should be noted that AGK +81 266 was observed using the F28x50LP “long-pass” filter rather than the F25ND3 filter which was used for the η Carinae observations. At the same time, the gross spectral energy distribution of AGK +81 266 (spectral class B5) and η Carinae are very dissimilar. This is not significant since AGK +81 266 is only used to demonstrate that this method

accurately measures a constant brightness over the temporal baseline for an established flux standard. The brightness of η Carinae is *not* measured relative to AGK +81 266.

2.1.3. Results

In Figure 4 and Table 2 we present our results for the STIS acquisition images as instrumental magnitudes calibrated for long term sensitivity effects using the photometric constants calculated by the reduction pipeline (Kim Quijano et al. 2003) and scaled relative to the value on 1999 February 20 (1999.14). These represent an extremely broad-band wavelength sample (Figure 1). For the purpose of comparison with familiar photometric systems, Table 1 gives approximate Johnson V (Johnson & Morgan 1953) and Cousins R and I (Cousins 1976) magnitudes at the reference epoch (1999.14). These were calculated using flux-calibrated STIS spectroscopic data (Davidson et al. 2003), a flux-calibrated spectrum of Vega (Colina, Bohlin, & Castelli 1996), and the appropriate response functions (Johnson & Morgan 1951; Bingham & Cousins 1974). For reasons noted in Section 1 and uncertainties in the STIS slit throughput for an object which is not exactly a point source, entries for η Carinae in Table 1 probably have uncertainties of roughly ± 0.05 magnitudes and could possibly be somewhat worse. It is also possible that the photometric color may trend mildly blue-ward as the object brightens (Davidson et al. 1999b).

The Homunculus is currently of 5th magnitude according to *ground-based* Johnson V photometry (Section 3 below), but the central star is fainter than $V = 7.0$ as stated in Table 1. Its apparent continuum is red, while stellar-wind emission lines contribute a significant fraction of its brightness. In the 1999.14 spectrum, $H\alpha$ and other emission features contribute about 16% of the flux in V (4% from $H\alpha$) and 38% of the flux in R (35% from $H\alpha$). Meanwhile, there is about a 5% affect on the I flux from the Hydrogen Paschen lines which are in emission. Because these emission features are constantly changing, it is not possible to formulate a consistent set of transformations to convert the STIS magnitudes to more familiar Johnson V and Cousins R and I magnitudes for η Carinae. However, the values presented for 1999.14 can serve as a rough zero point.

Figure 4 shows that the dramatic brightening reported by Davidson et al. (1999b) leveled off by 2000, but may have resumed at least temporarily around the mid-2003 spectroscopic event. The dip in brightness near the time of the event (Figure 6) may be reminiscent of the near-infrared behavior reported by Feast, Whitelock, & Marang (2001). This will be discussed further in Section 4.

2.1.4. Concerning $H\alpha$ Emission

Eta Carinae’s broad $H\alpha$ emission, produced in the stellar wind at radii of several AU, is tremendously strong (equivalent width usually about 800 Å). This feature did not vary much relative to the continuum in STIS data from 1998 to 2002, but recently it has faded to a surprising degree as reported below. Since $H\alpha$ contributes appreciably to the STIS acquisition images, we have investigated the effects on our photometry.

Davidson (2003) has measured the equivalent width of $H\alpha$ and estimated the absolute level of the nearby continuum in short-exposure STIS slit data. $H\alpha$ was integrated from 6509 to 6650 Å, and the continuum flux was averaged between 6740 and 6800 Å (an interval that is practically uncontaminated by emission lines). These continuum measurements have the advantage of being approximately calibrated in physical units, but on the other hand may be underestimated if the slit was not perfectly centered on the star. Fortunately, the $H\alpha$ equivalent width measurements are quite insensitive to slit position. The results are shown in Figure 5. We estimate that $H\alpha$ contributes from 8% to 16% of the STIS/F25ND3 counts, varying with time as listed in Table 2. Open triangles in Figure 4 represent the instrumental magnitudes that would have been observed if $H\alpha$ were not present; evidently the brightness minimum in early 2003 and the subsequent rapid brightening are not due to this emission line. The measured brightness fluctuations in the central star appear to be mainly (though not entirely) changes in the continuum brightness.

In the six months preceding the 2003.5 event (December 2002 to June 2003), the equivalent width of $H\alpha$ declined by a factor of nearly 2, while its line profile evolved in an interesting and unexpected way which is beyond the scope of this paper. The other Balmer lines behaved in a similar fashion. Moreover, in July and September 2003 they did not return to the state observed by STIS in 1998 at the corresponding point in η Car’s 5.54-year cycle. A more in-depth account of these effects will be reported in a paper which is now in preparation (Davidson et al. 2004).

2.2. ACS/HRC Observations

HST ACS/HRS observations of η Car were obtained for the HST Treasury Project beginning in October 2002. Bias corrected, dark subtracted, and flat fielded ACS/HRC images were obtained from Space Telescope Science Institute via the Multi-mission Archive (MAST)². Observations which had overexposed the central star were not used and no drizzle

²<http://archive.stsci.edu/>

or dithering correction is applied.

The ACS/HRC images were taken in four filters which cover near UV and optical wavelengths (Figure 1). Each of these filters is influenced by different types of spectral features. The UV filters (HRC/F220W & HRC/F250W) are heavily influenced by the “Fe II forest” (Cassatella, Giangrande, & Viotti 1979; Altamore et al. 1986; Viotti et al. 1989). The opacity of this “forest” is known to dramatically increase during an event (Davidson, Ishibashi, Gull, & Humphreys 1999b; Gull, Davidson, & Ishibashi 2000). The HRC/F330W filter is sensitive to both the Balmer continuum and a number of emission features while the HRC/F550M filter, strategically placed between $H\alpha$ and $H\beta$, almost exclusively measures the continuum.

The relative brightness of the central star in the ACS/HRC images is measured with the same weighted 0.3 arcsecond diameter aperture used to measure the STIS acquisition images. On the scale of the ACS/HRC this corresponds to $R = 5$ pixels and includes about 79 pixels inside the aperture. The results are given in Table 3 and Figure 6. The magnitudes given are on the STMAG system (Holtzman et al. 1995) as calibrated by the photometric keywords calculated by the reduction pipeline (Pavlovsky et al. 2003). Note that the HRC/F220W and HRC/F250W curves show a significant dip at the time of the 2003.5 event, due to the Fe II absorption as noted above. Interestingly, the visual continuum measured by the HRC/F550M filter does *not* show the decrease in brightness seen at longer wavelengths in the STIS data.

3. Ground-based AAVSO Data

While space-based photometry is able to resolve the central star, ground based photometry measures the integrated brightness of both the star and the Homunculus nebula. However, ground-based photometry is still valuable because it has a longer temporal baseline and shows many of the same brightness variations, albeit at different amplitudes. Also as more publicly funded small telescopes are closed the data from the AAVSO and groups like La Plata observatory (Fernandez Lajus et al. 2003) will become increasingly useful for monitoring objects like η Car.

One of the few sources for long term monitoring of η Carinae is the American Association of Variable Star Observers (AAVSO) (Mattei & Foster 1998). From 1968 through mid-2003 there are 6640 observations from 110 observers situated around the globe³. These data are from individual observers who have determined the brightness of η Carinae by visually

³<http://www.aavso.org/news/etacar.shtml>

comparing it with the brightness of other stars. Ten observers account for 69% of these observations while 36% of the observations are from the two most prolific observers: M. Daniel Overbeek (Mattei & Fraser 2003) and Albert F. Jones. On average, there are 60 observations per observer but the median is 9 observations per observer.

We averaged the observations in 90 day bins with a median of 32 observations in each bin. The bottom panel of Figure 7 shows binned averages from 1968 through mid 2003 with a typical standard deviation of 0.2 magnitudes, which is consistent with the accepted usual r.m.s. error of 0.1 – 0.2 magnitudes for observations of this type. The top panel of Figure 7 shows the photoelectric Johnson V band photometry (PEPV) from Stan Walker (Davidson et al. 1999b), photoelectric observations from R. Winfield Jones obtained through the AAVSO, and the average V_J magnitude from ground based observations reported in Figure 2 of Davidson et al. (1999b). The data in both panels follow the same general trend and compare well with the data presented in Figure 2 of Sterken, de Groot, & van Genderen (1996). Even the most primitive AAVSO data track the professional photometry well enough to show irregular behavior. The maximum noted by Sterken, de Groot, & van Genderen (1996) at 1982.11 is visible in all the data, though the errors in the binned AAVSO data make it harder to recognize. Each dataset also shows an overall brightening trend in η Carinae over the past thirty years along with a notable jump in brightness in 1998-1999 (Davidson et al. 1999b).

The binned AAVSO data for the last five years (Figure 8) also follows a trend similar to the brightness variations in the central star measured from the STIS acquisition images (Figure 4). Of particular note, both datasets show the brightening of η Carinae peaked in 2000, fell off a bit, and then peaked again in early 2002 before brightening through the 2003.5 event.

4. Analysis & Conclusions

The data presented here from the HST and ground-based observations confirm the dramatic brightening in both the nebula and central star of η Carinae which was previously reported by Davidson et al. (1999a,b) and Sterken, Freyhammer, Arentoft, & van Genderen (1999) along with a more gradual brightening spanning the past thirty years. All the available data also show that the apparent brightness of η Carinae fluctuates with no obvious period. We also see intervals (on the order of months) with short lived increases in apparent brightness similar to those reported by van Genderen, Sterken, & Allen (2003a). The 2003.5 event, as observed in the brightness fluctuations of the central star at visual wavelengths, was characterized by a roughly six month rise, then a sharp dip in most filters, followed by

a recovery to the highest flux observed for the central star in recent years, which may be the start of another significant brightening episode. Again we emphasize that since 1997 *the central star has brightened substantially faster than the Homunculus* (compare Figures 4 and 7).

The STIS, ACS, $H\alpha$, and AAVSO data all have notable trends which began about 200 days before the 2003.54 event. The visual band photometry from the STIS, ACS, and AAVSO began to brighten significantly in January 2003 (Figures 9 & 6 and also Fernandez Lajus et al. (2003)) which coincided with a steep drop in $H\alpha$ luminosity (Figure 5) and the beginning of a dip in brightness in the near-UV (Figure 6). The start time for this pre-event activity is important because most models which invoke a binary companion to trigger the events place the secondary on a very eccentric orbit where it is in close proximity to the primary for only a very brief period of time during each cycle. Feast, Whitelock, & Marang (2001) showed that the J , H , K and L bands brightened roughly 500 days before the time of the events over the past two decades with an additional sharp rise in the J , H , and K bands about 80 days prior to the 1998.0 event. The X-ray flux from η Car (Ishibashi et al. (1999) and M. Corcoran’s web page⁴ for data on the recent event) also increased before the 1998.0 and 2003.54 events, preceding them by about 350 and 700 days respectively. It is not necessary or expected that all of the pre-event activity will temporally coincide since each of these data measure activity which occurs at different radii from the star and a shock front which pushes deeper as the event proceeds will not affect each process simultaneously. Also, as noted below there is compelling evidence that the state and distribution of the material immediately surrounding the central star has evolved over time so while the activity prior to the event should maintain roughly the same sequential order, the exact start times relative to the event could potentially change from cycle to cycle.

The ACS/HRC data show that the brief dip in apparent brightness during the 2003.5 event is not achromatic. The ACS data show that the depth of the dip is wavelength dependent; the dip is deeper at shorter wavelengths and the brightness continually increased in the HRC/F550M filter through the last data point. However, Feast, Whitelock, & Marang (2001) showed that the brief decrease or dip in luminosity occurred at all of the near-IR wavelengths during the 1998.0 event (Figure 9, reproduced from Feast, Whitelock, & Marang (2001)) and Whitelock, Marang, & Crause (2003) reported similar activity during the 2003.5 event. This leaves two possibilities which are not mutually exclusive:

1. The decrease in brightness occurs later at redder wavelengths and/or

⁴http://lheawww.gsfc.nasa.gov/users/corcoran/eta_car/etacar_rxte_lightcurve/

2. The decrease in brightness is driven entirely by increased line opacities, decreased emission lines, and Balmer and Paschen continua formed in the wind, rather than a change in the star’s continuum flux.

Feast, Whitelock, & Marang (2001) show that during the 1998.0 event, the dip in the J band occurred about 35 days later than the dip in the X-Rays. They also note that the epoch of the minimum in the dip increases slightly with increasing effective wavelength (Figure 9). Whitelock, Marang, & Crause (2003) reported that during the 2003.5 event the dip in the J and L bands began sometime between MJD 52809.5 (2003.467) and 52814.5 (2003.481), which preceded the observed dip in Johnson-Cousins $BVRI$ by about one to two weeks (Fernandez Lajus et al. 2003; van Genderen, Sterken, Allen, & Liller 2003b). (Note that wavelengths around $2\ \mu\text{m}$ observed by Feast, Whitelock, & Marang (2001) presumably represent free-free emission in the wind at radii substantially larger than the photosphere at visual wavelengths.) Given only the HST data, one might suspect that dip in the HRC/F550M filter may have occurred between data points and the slight rise observed at MJD 52803.1 (2003.45) is the rise in luminosity which precedes the dip. However, the HRC/550M observation at MJD 52840.1 (2003.55) shows a *rise* in flux roughly coincident with the minimum observed in $BVRI$ by Fernandez Lajus et al. (2003) and van Genderen, Sterken, Allen, & Liller (2003b). Therefore, it is unlikely that we missed the dip in HRC/550M due to sampling.

Likewise, strong P-Cygni absorption is present in the hydrogen lines during the event (Davidson, Ishibashi, Gull, & Humphreys 1999b). Since the hydrogen emission lines contribute significantly to the total brightness of the central star, anything that changes their profiles will change the brightness measured in a filter which they influence. The HRC/F550M filter covers none of the prominent emission lines and it shows no dip concurrent with the dip in the other filters. Therefore, this may indicate that the bolometric luminosity of the central star is largely unaffected by the mechanism which causes the observed decrease in brightness.

Davidson et al. (1999b) discuss several possible explanations for the variability in the brightness of the central star of η Carinae. Since the star itself radiates near the Eddington Limit, there is little room for rapid or dramatic changes in bolometric luminosity. This is supported by the fact that the surrounding nebula, which acts as a giant calorimeter for the central star, varies in brightness on a significantly smaller scale. If the bolometric luminosity of the central star stays roughly constant, then significant variations in its brightness may be more appropriately interpreted as changes in the density, temperature, and spatial distribution of intervening circumstellar material. An expanding shell of ejecta from an event may be able to produce the observed light curves (Zanella, Wolf, & Stahl 1984; Davidson, Ishibashi,

Gull, & Humphreys 1999b; Davidson et al. 1999b; Smith et al. 2003). Any ejected shell should start hot with high opacities from ionized metals and then later shift these opacities to the red as the shell cools and dust forms. Particularly at early stages, this shell may be optically thin and as such would not have a significant impact on the continuum brightness.

The data show that central star of η Carinae continues to brighten. We are unsure how long this trend can continue but it appears to be driven by an increase in the apparent continuum brightness which may be caused by changes in the intervening circumstellar material along the line of sight, although how or why the circumstellar material may have been altered is not completely understood. Continued monitoring is critical since coming out of the 2003.5 event there are indications that the central star may undergo another period of sudden dramatic brightening in the near future.

The brief decrease in the star’s brightness during the 2003.5 event was more complicated than expected and changes preceding the event in the optical and near-UV started as early as January 2003. The wavelength dependence of the dip indicates that it cannot be caused by a simple eclipse or occultation. If the primary star is eclipsed by the presumed secondary we would expect to observe some decrease at all wavelengths including the HRC/550M band which measures the continuum. On the other hand if an eclipse of the secondary is sufficient to cause a dip of approximately 0.5 mag in the near UV flux of the central star, then we would expect to find some spectroscopic evidence for the secondary in the HST/STIS spectra during the 5.5 year cycle which is not the case. However, the data may support a shell ejection model for the spectroscopic events. Additional data, including spectra gathered by the STIS during the 2003.5 event, should further constrain the mechanism powering these periodic phenomena.

5. Acknowledgments

This research was conducted as part of the HST Treasury Project on η Carinae via grant no. GO-9420 from the Space Telescope Science Institute. We acknowledge Kris Davidson, Roberta M. Humphreys, and Kazunori Ishibashi for directly assisting with the data and measurements and T.R. Gull for preparing most of the HST observing plans. Other participants in the HST Treasury Project are D. John Hillier, Augusto Damineli, Michael Corcoran, Otmar Stahl, Kerstin Weis, Sveneric Johansson, Fred Hamann, H. Hartman, Nolan Walborn, and Manuel Bautista.

We are also grateful to the AAVSO International Database for the variable star observations contributed by observers worldwide. We individually thank Janet A. Mattei and

Elizabeth O. Waagen of the AAVSO who helped us obtain the data and Stan Walker and R. Winfield Jones who provided photoelectric photometry data. We are very appreciative of M. Feast, and P. Whitelock for allowing us to reproduce their figures. And we thank Matt Gray and Qian An for providing the η Carinae project with computer technical support.

REFERENCES

- Altamore, A., Baratta, G. B., Cassatella, A., Rossi, L., & Viotti, R. 1986, *New Insights in Astrophysics. Eight Years of UV Astronomy with IUE*, 303
- Bingham, R. G. & Cousins, A. W. J. 1974, *Monthly Notes of the Astronomical Society of South Africa*, 33, 15
- Bohlin, R. C., Dickinson, M. E., & Calzetti, D. 2001, *AJ*, 122, 2118
- Cassatella, A., Giangrande, A., & Viotti, R. 1979, *A&A*, 71, L9
- Clampin, M., Hartig, G., Baum, S., Kraemer, S. Kinney, E. Kutina, R., Pitts, R., & Balzano, V./ 1996, *STIS Instrument Science Report 96-030*, (Baltimore, STSci)
- Colina, L., Bohlin, R., & Castelli, F. 1996, *Instrument Science Report CAL/SCS-008*, (Baltimore, STSci)
- Cousins, A. W. J. 1976, *Mem. R. Astr. Soc.*, 81, 25
- Damineli, A. 1996, *ApJ*, 460, L49
- Davidson, K. & Humphreys, R. M. 1997, *ARA&A*, 35, 1
- Davidson, K., Humphreys, R. M., Ishibashi, K., Gull, T. R., Hamuy, M., Berdnikov, L., & Whitelock, P. 1999a, *IAU Circ.*, 7146, 1
- Davidson, K. et al. 1999b, *AJ*, 118, 1777
- Davidson, K., Ishibashi, K., Gull, T. R., & Humphreys, R. M. 1999b, *ASP Conf. Ser.* 179: *Eta Carinae at The Millennium*, 227
- Davidson, K. 2000, *Cosmic Explosions: Tenth Astrophysics Conference. AIP Conference Proceedings*, Vol. 522. College Park, Maryland, 11-13 Oct 1999. Edited by Stephen S. Holt and William W. Zhang. American Institute of Physics, 2000., p.421-430, 421
- Davidson, K. et al. 2003, personal communication

- Davidson, K. et al. 2004, AJ, in preparation
- Davis, M., Campbell, D., Sticka, R., Faful, B. Leidecker, H., Kimbel, R., & Goudfrooij, P. 2001, STIS Failure Review Board Final Report (Baltimore: STSci)
- Downes, R., Clampin, M., Shaw, R., Baum, S., Kinney, E. & McGrath, M. 1997, STIS Instrument Science Report 97-03B, (Baltimore, STSci)
- Feast, M., Whitelock, P., & Marang, F. 2001, MNRAS, 322, 741
- Fernandez Lajus, E., Gamen, R., Schwartz, M., Salerno, N., Llinares, C., Farina, C., Amorn, R., & Niemela, V. 2003, Informational Bulletin on Variable Stars, 5477, 1
- Gull, T. R., Davidson, K., & Ishibashi, K. 2000, Cosmic Explosions: Tenth Astrophysics Conference. AIP Conference Proceedings, Vol. 522. College Park, Maryland, 11-13 Oct 1999. Edited by Stephen S. Holt and William W. Zhang. American Institute of Physics, 2000., p.439-442, 439
- Holtzman, J. A., Burrows, C. J., Casertano, S., Hester, J. J., Trauger, J. T., Watson, A. M., & Worthey, G. 1995, PASP, 107, 1065
- Ishibashi, K., Davidson, M. F., Corcoran, K., Drake, S. A., Swank, J. H., & Petre, R. 1999, ASP Conf. Ser. 179: Eta Carinae at The Millennium, 266
- Johnson, H. L. & Morgan, W. W. 1953, ApJ, 117, 313
- Johnson, H. L. & Morgan, W. W. 1951, ApJ, 114, 522
- Mattei, Janet & Fraser, Brian 2003, JAAVSO, 31, 65
- Mattei, Janet & Foster, G. 1998, IAPPP Communications, 72, 53
- Pavlovsky, C., et al. 2003, ACS Instrument Handbook, Version 4.0, (Baltimore: STSci)
- Proffitt, C. R. et al. 2002, The 2002 HST Calibration Workshop : Hubble after the Installation of the ACS and the NICMOS Cooling System, Proceedings of a Workshop held at the Space Telescope Science Institute, Baltimore, Maryland, October 17 and 18, 2002. Edited by Santiago Arribas, Anton Koekemoer, and Brad Whitmore. Baltimore, MD: Space Telescope Science Institute, 2002., p.97, 97
- Kim Quijano, J., et al. 2003, STIS Instrument Handbook, Version 7.0, (Baltimore: STSci)
- Smith, E., Stys, D., Walborn, N., & Bohlin, R. 2000, Instrument Science Report STIS 2000-03, (Baltimore: STSci)

- Smith, N., Davidson, K., Gull, T. R., Ishibashi, K., & Hillier, D. J. 2003, *ApJ*, 586, 432
- Sterken, C., de Groot, M. J. H., & van Genderen, A. M. 1996, *A&AS*, 116, 9
- Sterken, C., Freyhammer, L., Arentoft, T., & van Genderen, A. M. 1999, *A&A*, 346, L33
- Sterken, C., Freyhammer, L. M., Arentoft, T., & van Genderen, A. M. 2001, *ASP Conf. Ser.* 233: *P Cygni 2000: 400 Years of Progress*, 39
- Stys, D. J. & Walborn, N. R. 2000, *Instrument Science Report STIS 2001-01R*, (Baltimore, STSci)
- van Genderen, A. M., de Groot, M. J. H., & The, P. S. 1994, *A&A*, 283, 89
- van Genderen, A. M. et al. 1995, *A&A*, 304, 415
- van Genderen, A. M., Sterken, C., de Groot, M., & Burki, G. 1999, *A&A*, 343, 847
- van Genderen, A. M., Sterken, C., & Allen, W. H. 2003a, *A&A*, 405, 1057
- van Genderen, A. M., Sterken, C., Allen, W. H., & Liller, W. 2003b, *A&A*, 412, L25
- Viotti, R., Rossi, L., Cassatella, A., Altamore, A., & Baratta, G. B. 1989, *ApJS*, 71, 983
- Whitelock, P. A., Feast, M. W., Koen, C., Roberts, G., & Carter, B. S. 1994, *MNRAS*, 270, 364
- Whitelock, P. A., Marang, F., & Crause, L. 2003, *IAU Circ.*, 8160, 2
- Zanella, R., Wolf, B., & Stahl, O. 1984, *A&A*, 137, 79

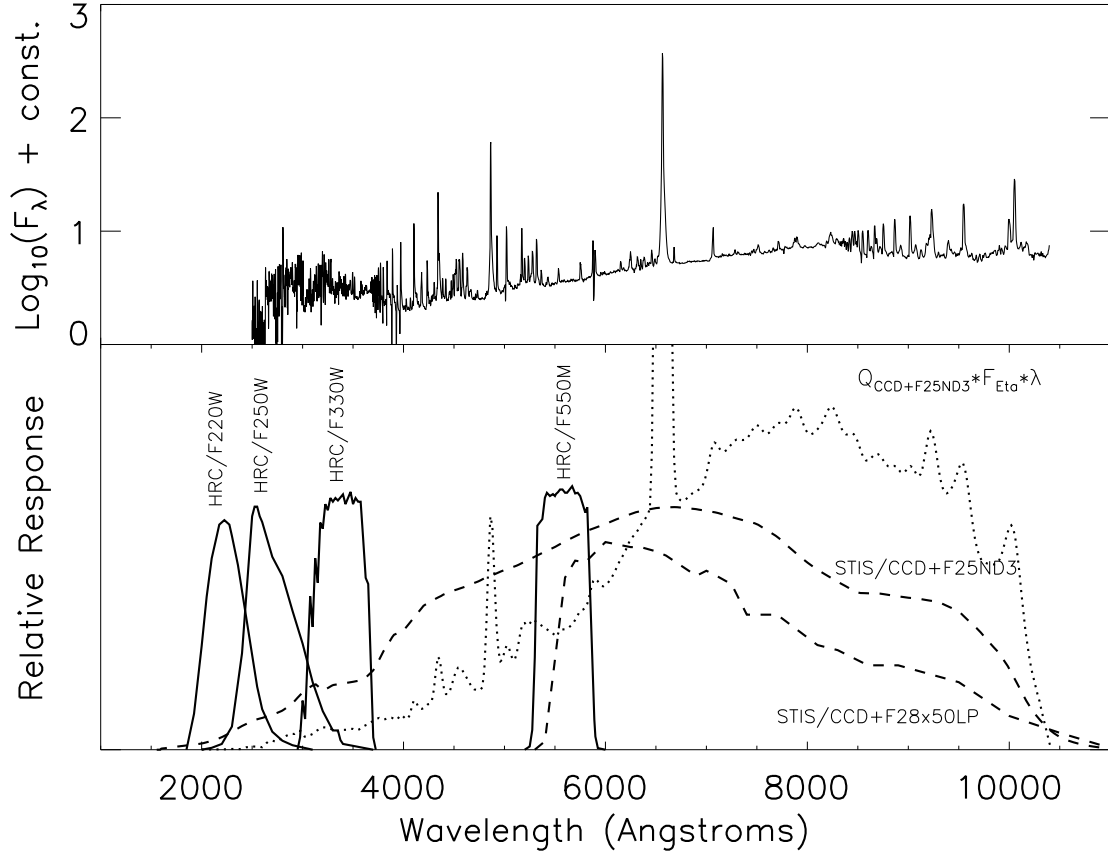


Fig. 1.— The top panel shows the relative spectral flux from the central star of η Carinae. The bottom panel shows the total relative response of each CCD and filter combination used in this study on the same wavelength scale as the top panel. For plotting purposes the curves are not representative of relative responses between filters. STIS filters are plotted with a dashed line and ACS/HRC filters are plotted with a solid line. The dotted line represents the product of the STIS CCD+F25ND3 response curve and the photon flux from the central star.

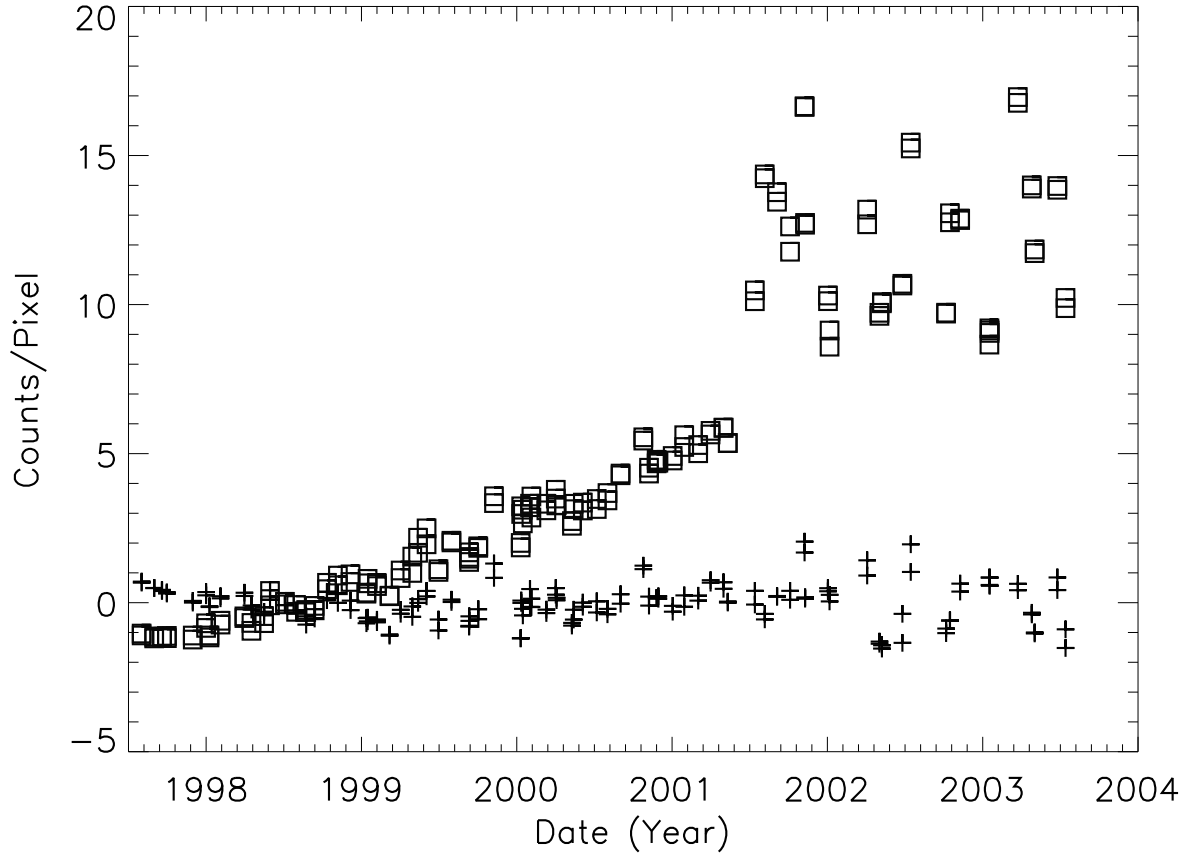


Fig. 2.— A plot of the residual bias level in the 80 STIS acquisition image pairs of flux standard AGK +81 266. Open squares are the residual bias level before subtracting the modeled correction. Crosses (+) are the bias level after subtracting the modeled correction.

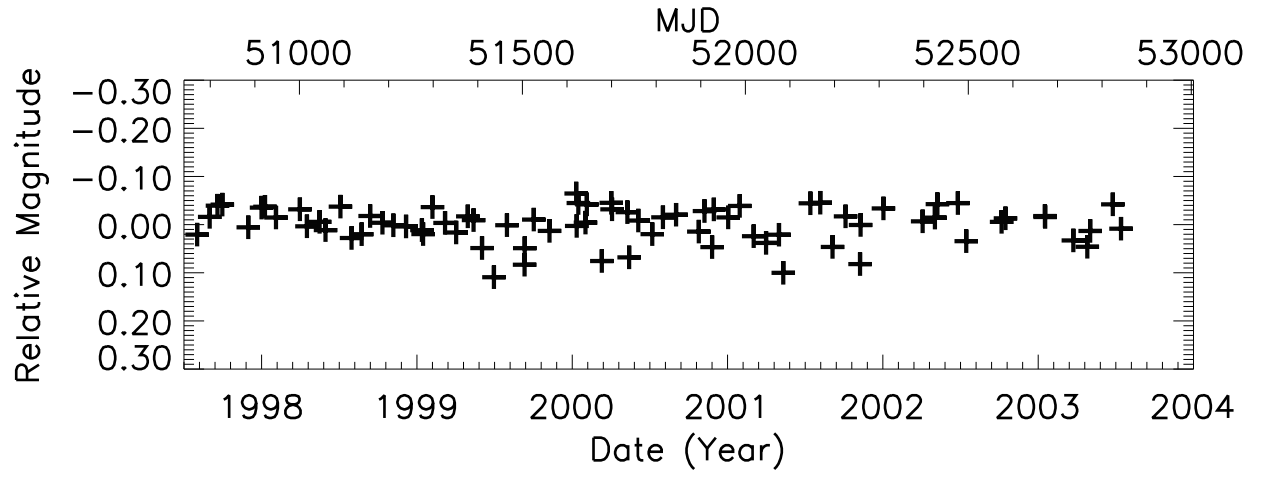


Fig. 3.— The relative brightness of flux standard AGK +81 266 measured using a 0.3 arcsecond diameter weighted aperture.

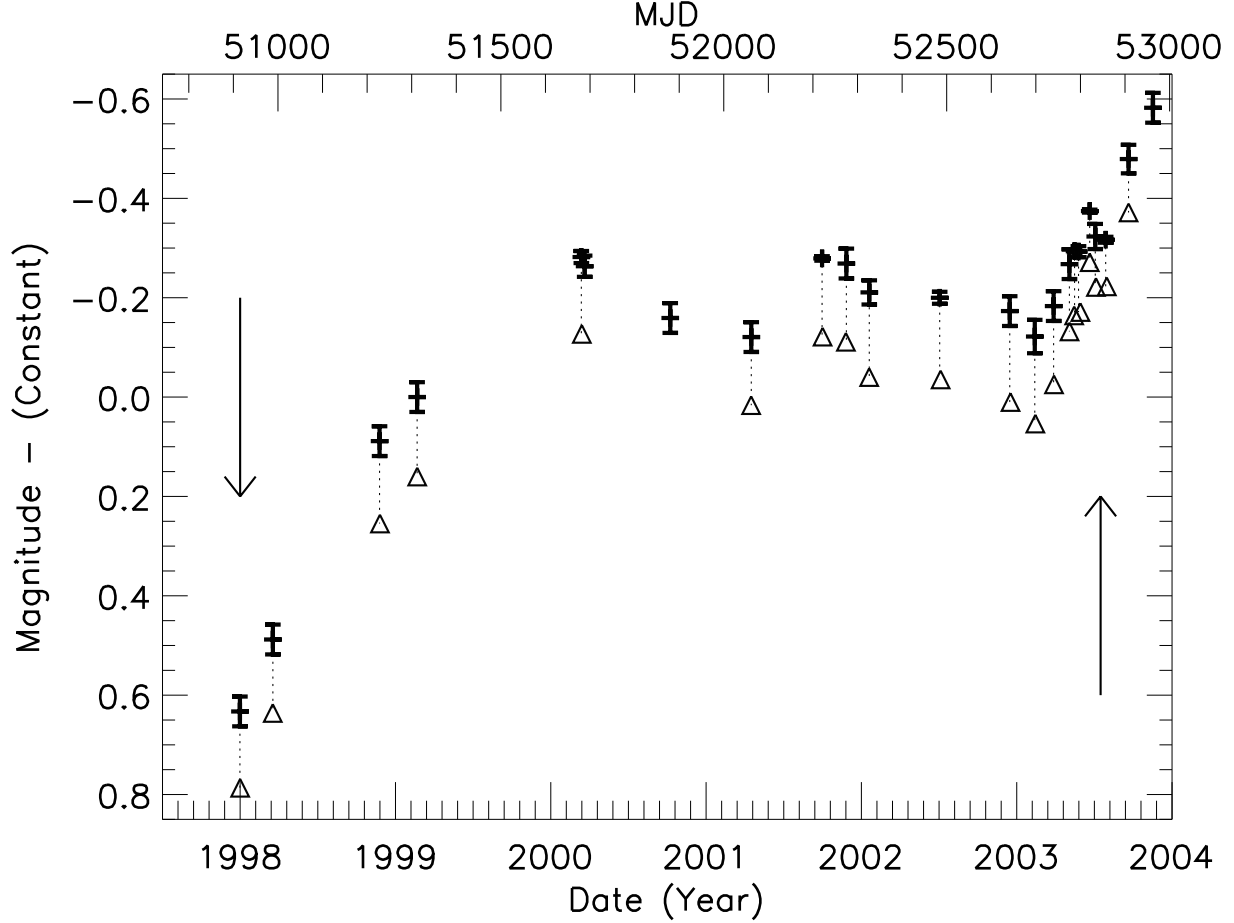


Fig. 4.— The crosses (+) with error bars are the average relative brightness of the central star in the STIS acquisition images (Table 2). The error bars are the one sigma standard deviation of the measurements included in each point. The error bars plotted for points including only one measurement are the r.m.s. deviation of the brightness measured for the flux standard AGK +81 266. The open triangles are the magnitudes with the contribution of $H\alpha$ subtracted. Vertical arrows mark the times of the 1998.0 and 2003.54 spectroscopic events. See Figure 6 for an expanded view of the data around the 2003.5 event.

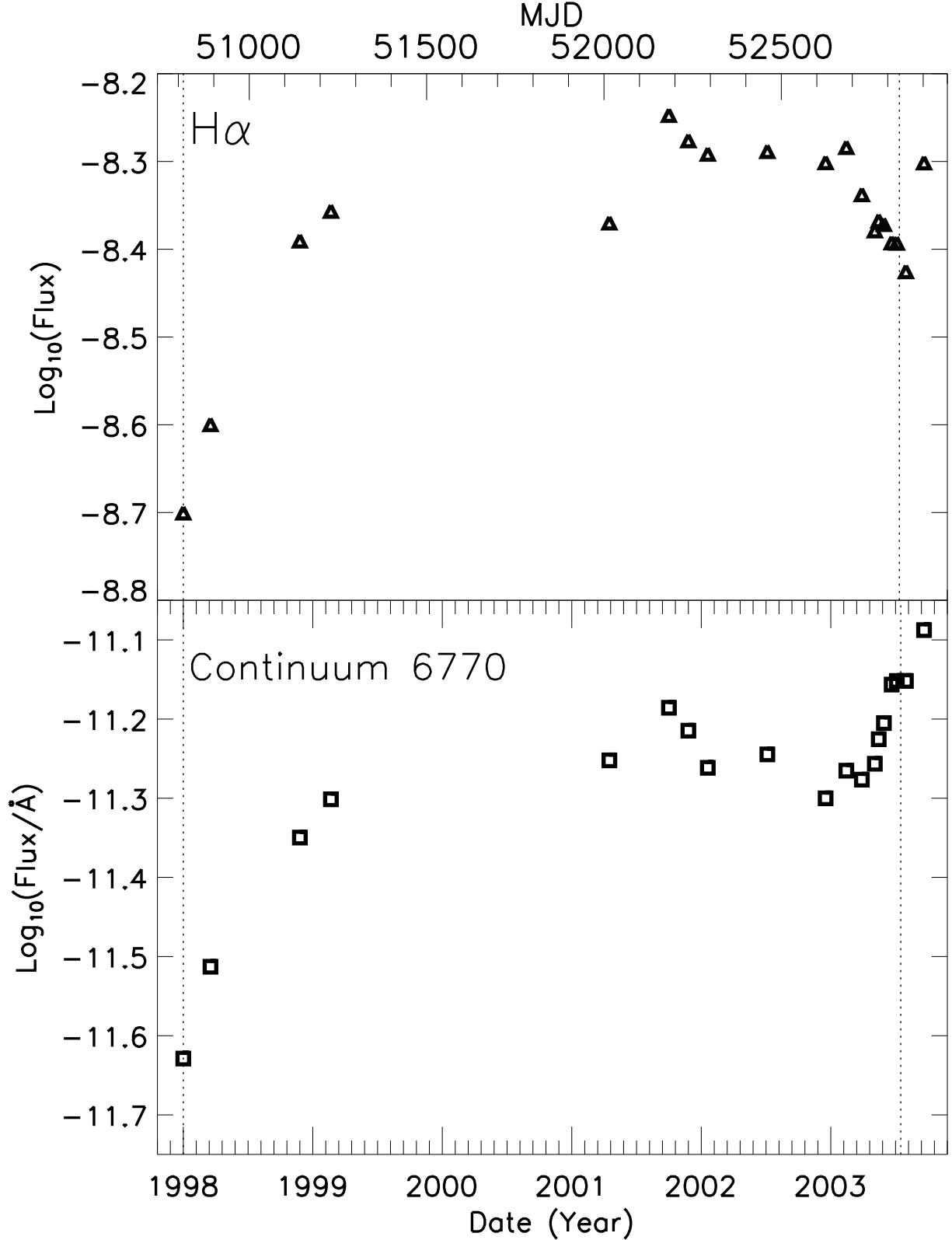


Fig. 5.— The flux of features in the STIS spectrum of the central star. The top panel shows the log of the total integrated flux of H α in $\text{erg}/\text{cm}^2/\text{s}$. The bottom panel shows the log of the continuum flux measured at 6770 \AA in $\text{erg}/\text{cm}^2/\text{s}/\text{\AA}$. The dotted vertical lines mark the spectroscopic events at 1998.0 and 2003.54.

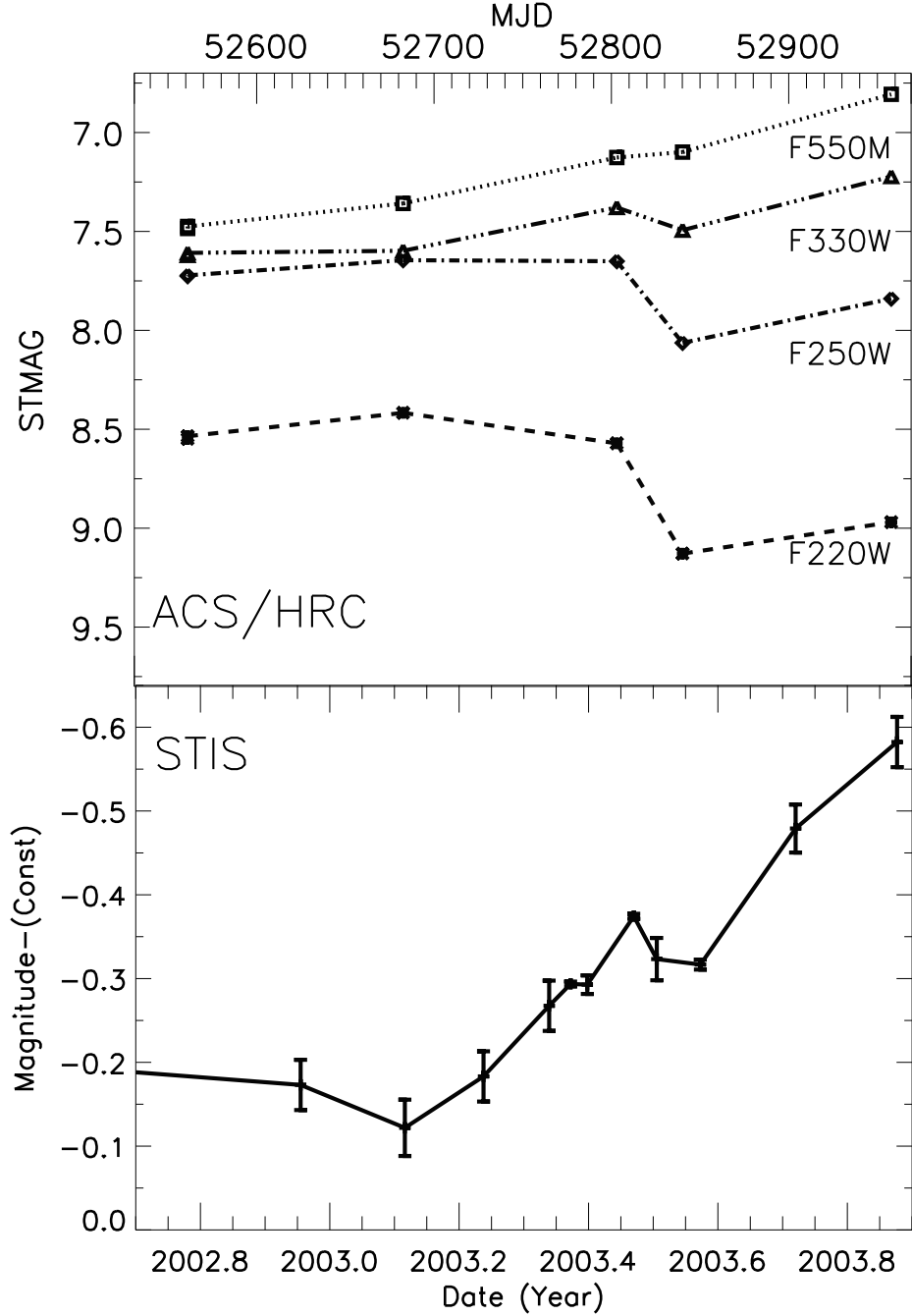


Fig. 6.— The top panel shows the brightness of central star in the ACS/HRC images with each point representing the average from several individual exposures (Table 3). The data for each filter is represented as its own line, labeled on the right. The bottom panel shows the data from the STIS acquisition images (solid line).

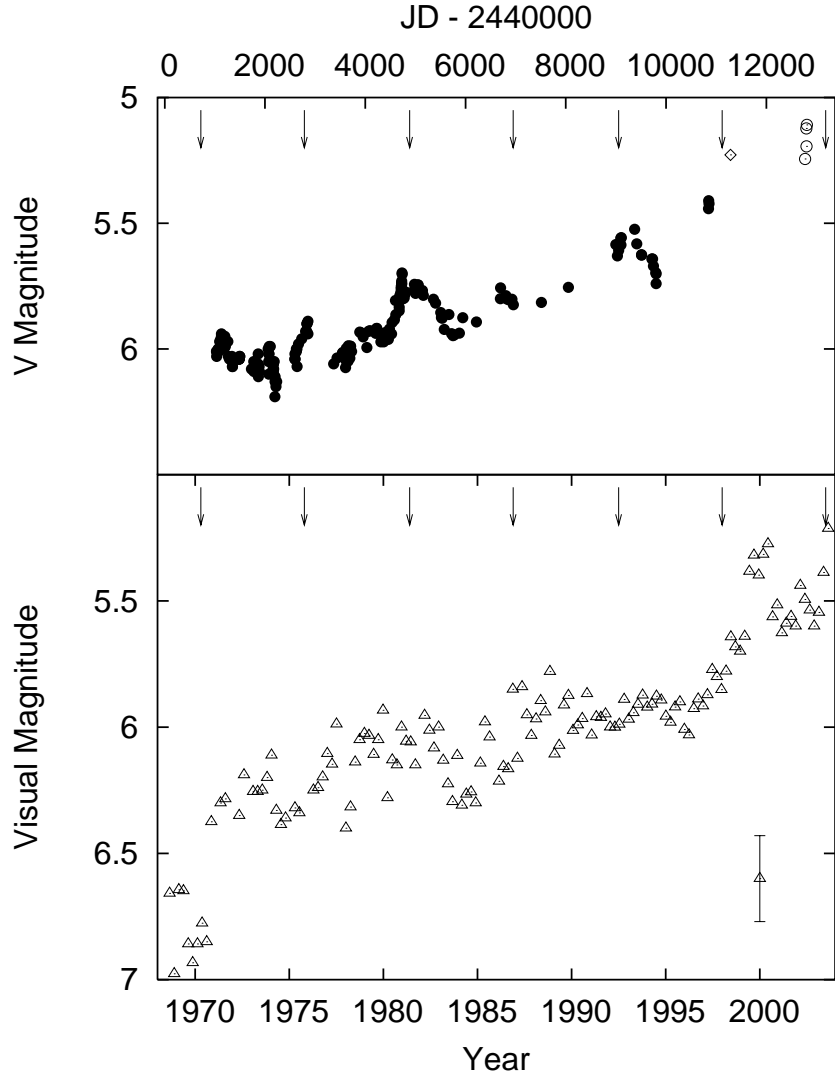


Fig. 7.— The light curve of η Carinae from ground based observations. The top graph shows the photoelectric V magnitudes (PEPV) from Stan Walker (filled circles), photoelectric V observations by R. Winfield Jones obtained from the AAVSO (open circles), and the average V_J magnitude from the ground based observations reported by Davidson, Ishibashi, Gull, & Humphreys (1999b) (open diamond). The bottom panel shows the averages of the visual AAVSO observations in bins of 90 days. A representative error bar for the binned AAVSO observations is shown in the lower right; see also Fig. 8. The arrows along the top of each panel mark the interval of past events with the 5.54-year period adopted in 2001 for the Treasury Project proposal. This period was based on photometric details reported by Feast, Whitelock, & Marang (2001) and various other data, and it predicted the timing of the 2003 event quite well.

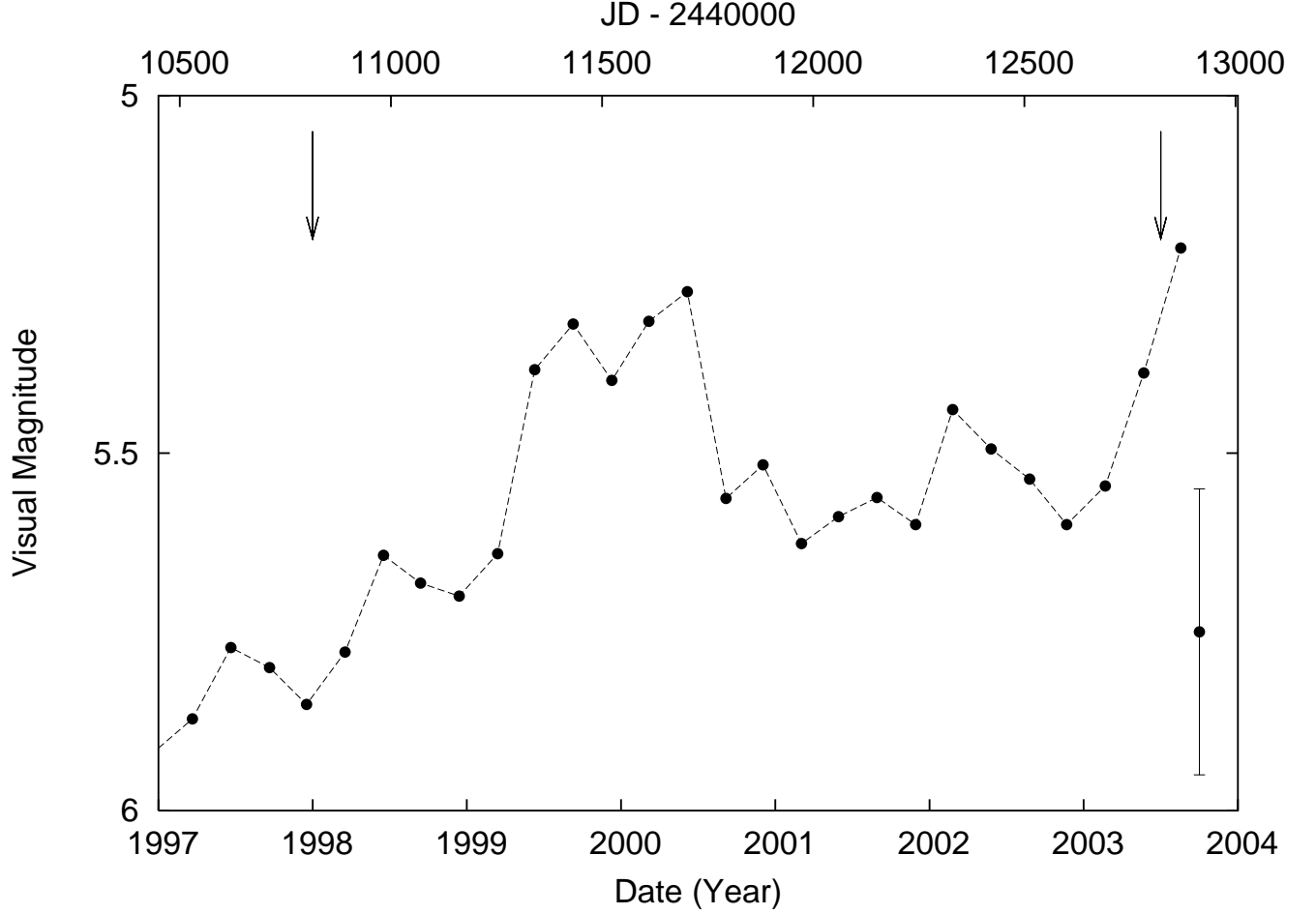


Fig. 8.— Eta Car light curve from 1997 through 2003 of the visual AAVSO observations averaged in bins of 90 days. A representative error bar for a single observation is shown in the lower right; each point here represents typically about 32 observations. The arrows on the top of the plot mark the 1998.0 and 2003.54 spectroscopic events. Formal error estimates are not fully justified in this case, but the r.m.s. uncertainty for each plotted point is probably about 20% as large as the single-observation error bar.

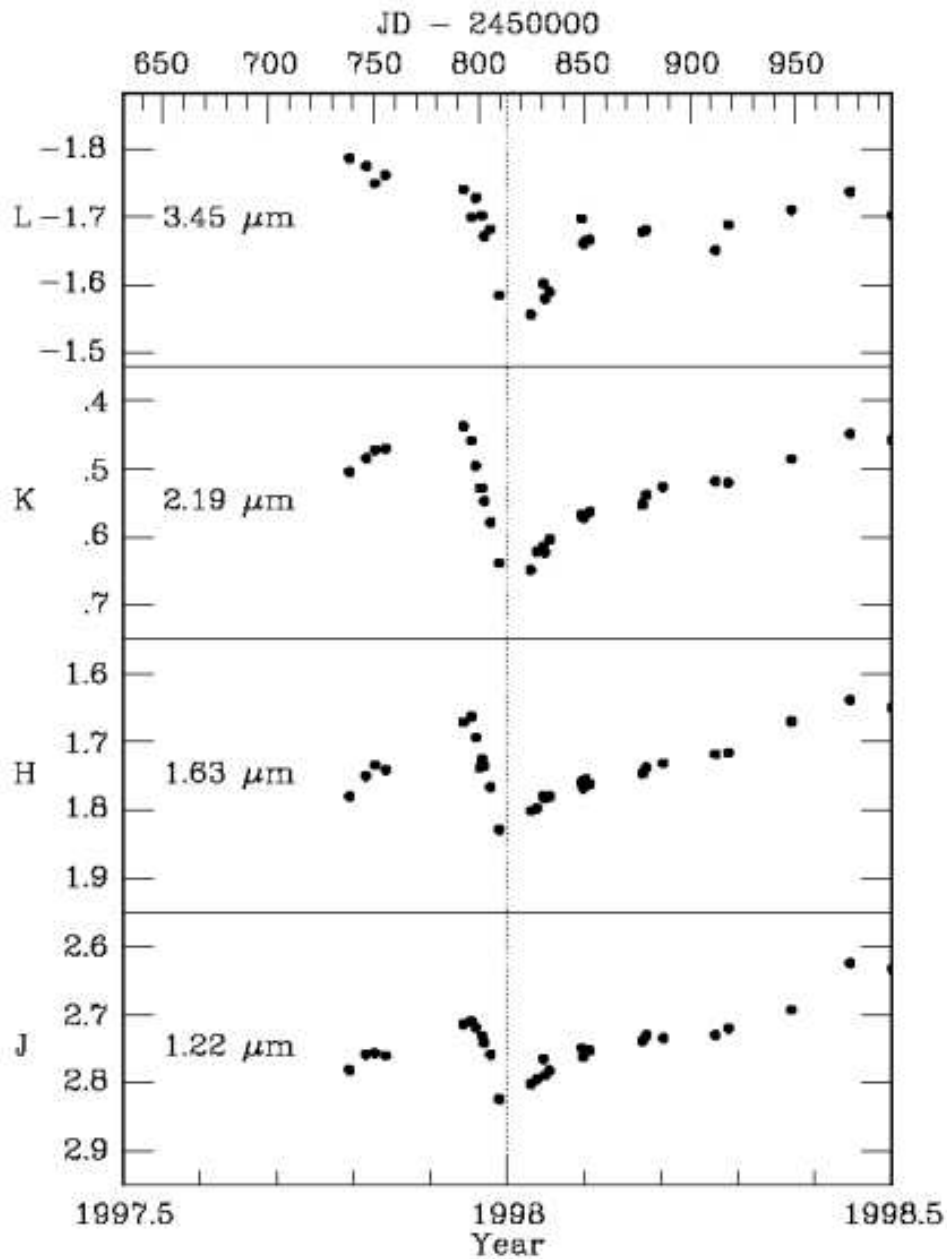


Fig. 9.— Figure 4 from Feast, Whitelock, & Marang (2001) reproduced with permission of the authors. Infrared light curves in $JHKL$ near the time of the 1998 "dip." The minimum of the dip (phase 0.977) is shown by the vertical line.

Table 1. Brightness of the Central Star at 1999.140

	V_J	R_C	I_C
η Car	7.73	6.11	4.47
Vega	0.030	0.021	0.025

Table 2. Results from STIS Acquisition Images

Dataset	MJD	Year	Flux ^c	% in H α ^d	Flux @ 6770 Å ^e	Magnitude ^a	Average ^b	σ ^b	Minus H α ^f
o4j802qxq	50814.008	1997.999	3.196E-12	13.2	2.35E-12	0.65	0.65	...	0.79
o4j801y4q	50891.414	1998.211	3.720E-12	12.7	3.07E-12	0.49	0.49	...	0.64
o55601hkq	51142.172	1998.898	5.374E-12	14.2	4.47E-12	0.09	0.09	...	0.25
o55602qsq	51230.449	1999.140	5.831E-12	13.7	5.00E-12	-0.00	-0.00	...	0.16
o5f102bkq	51616.484	2000.197	7.476E-12	13.3	...	-0.27	-0.28	0.01	-0.13
o5kz01coq	51623.785	2000.217	7.645E-12	-0.29
o5kz02gbq	51624.285	2000.218	7.580E-12	-0.28	-0.26	0.02	...
o5f101yoq	51626.762	2000.225	7.288E-12	-0.24
o5f103a1q	51826.039	2000.769	6.753E-12	-0.16	-0.16
o62r01h0q	52016.734	2001.291	6.518E-12	11.9	5.60E-12	-0.12	-0.12	...	0.02
o6ex03a9q	52183.086	2001.747	7.573E-12	13.5	6.52E-12	-0.28	-0.28	0.00	-0.12
o6en01c2q	52183.297	2001.747	7.509E-12	-0.27
o62r02fvq	52240.070	2001.903	7.470E-12	13.5	6.10E-12	-0.27	-0.27	...	-0.11
o6ex02tkq	52293.977	2002.051	7.241E-12	14.5	5.47E-12	-0.24	-0.21	0.02	-0.04
o6ex01wyq	52294.207	2002.051	6.923E-12	-0.19
o6mo02eaq	52459.480	2002.504	6.933E-12	14.1	5.69E-12	-0.19	-0.20	0.01	-0.04
o6mo01k6q	52459.781	2002.505	7.089E-12	-0.21
o8gm01a1q	52624.043	2002.955	6.840E-12	15.5	5.01E-12	-0.17	-0.17	...	0.01
o8gm12ukq	52682.859	2003.116	6.730E-12	14.9	5.43E-12	-0.16	-0.12	0.03	0.05
o8gm11zpq	52683.242	2003.117	6.326E-12	-0.09
o8gm21t9q	52727.234	2003.238	6.904E-12	13.5	5.29E-12	-0.18	-0.18	...	-0.03
o8gm41eqq	52764.266	2003.339	7.462E-12	11.7	5.54E-12	-0.27	-0.27	...	-0.13
o8gm33qsq	52776.398	2003.372	7.662E-12	11.2	5.95E-12	-0.30	-0.29	0.00	-0.16
o8gm32c6q	52778.469	2003.378	7.623E-12	-0.29
o8gm31fnq	52785.797	2003.398	7.617E-12	10.6	6.24E-12	-0.29	-0.29	0.01	-0.17
o8gm51fuq	52791.035	2003.412	7.752E-12	-0.31
o8gm52kyq	52791.707	2003.414	7.558E-12	-0.28
o8gm63ohq	52812.031	2003.470	8.264E-12	9.0	6.98E-12	-0.38	-0.37	0.00	-0.27
o8gm61pxq	52812.250	2003.471	8.212E-12	-0.37
o8gm62dwq	52813.703	2003.475	8.222E-12	-0.37
o8ma71jmq	52825.020	2003.506	7.675E-12	8.9	7.05E-12	-0.30	-0.32	0.03	-0.22
o8ma72liq	52825.355	2003.506	8.043E-12	-0.35
o8ma81mtq	52849.594	2003.573	7.763E-12	8.3	7.05E-12	-0.31	-0.32	0.01	-0.22
o8ma82b8q	52851.906	2003.579	7.850E-12	-0.32
o8ma91ubq	52903.355	2003.720	8.830E-12	-0.45	-0.48	0.03	...
o8ma92ctq	52904.289	2003.723	9.309E-12	-0.51
o8ma83fzq	52960.590	2003.877	9.969E-12	-0.58

^aRelative STIS magnitude in the F25ND3 filter zeroed on 1999.140

^bThe average and sigma of individual measurements within one day of each other. These values are plotted in Figure 4.

^cBrightness measured in F25ND3 filter given as STIS flux units (erg/cm²/s/Å).

^dAn estimate of the percent of the total flux measured in the F25ND3 filter which is contributed by H α .

^eThe continuum flux measured at 6770 Å in absolute flux units of erg/cm²/s/Å.

^fRelative magnitude in the F25ND3 filter with the contribution from H α subtracted (open triangles in Figure 4).

Table 3. Results from ACS/HRC Images

Dataset	MJD	Year	Flux ^c	Magnitude ^a	Average ^b	σ^b
HRC/F220W Filter						
j8gm1aa7q	52561.039	2002.782	1.385E-12	8.547	8.549	0.011
j8gm1aa8q	52561.039	2002.782	1.402E-12	8.533
j8gm1aalq	52561.047	2002.782	1.366E-12	8.562
j8gm1aamq	52561.047	2002.782	1.375E-12	8.554
j8gm1abmq	52561.098	2002.782	1.426E-12	8.515	8.535	0.015
j8gm1abnq	52561.098	2002.782	1.404E-12	8.531
j8gm1abyq	52561.105	2002.782	1.394E-12	8.539
j8gm1abxq	52561.105	2002.782	1.374E-12	8.555
j8gm2as1q	52682.547	2003.115	1.562E-12	8.416	8.417	0.007
j8gm2as5q	52682.551	2003.115	1.574E-12	8.407
j8gm2asaq	52682.555	2003.115	1.555E-12	8.421
j8gm2asoq	52682.566	2003.115	1.549E-12	8.425
j8ma3adhq	52803.055	2003.445	1.316E-12	8.601	8.571	0.018
j8ma3adlq	52803.086	2003.445	1.372E-12	8.557
j8ma3adqq	52803.090	2003.445	1.373E-12	8.556
j8ma3ae3q	52803.152	2003.446	1.355E-12	8.570
j8ma4aqfq	52840.145	2003.547	8.093E-13	9.130	9.129	0.003
j8ma4aqj	52840.148	2003.547	8.069E-13	9.133
j8ma4aqq	52840.156	2003.547	8.109E-13	9.128
j8ma4ar2q	52840.168	2003.547	8.137E-13	9.124
j8ma6ayjq	52957.809	2003.869	9.216E-13	8.989	8.970	0.01
j8ma6aynq	52957.844	2003.869	9.531E-13	8.952
j8ma6az2q	52957.855	2003.869	9.385E-13	8.969
HRC/F250W Filter						
j8gm1aaaq	52561.039	2002.782	2.935E-12	7.731	7.726	0.011
j8gm1aabq	52561.043	2002.782	2.995E-12	7.709
j8gm1aaqq	52561.047	2002.782	2.910E-12	7.740
j8gm1aapq	52561.051	2002.782	2.951E-12	7.725
j8gm1abpq	52561.098	2002.782	2.985E-12	7.713	7.722	0.018
j8gm1abqq	52561.098	2002.782	3.022E-12	7.699
j8gm1ac0q	52561.105	2002.782	2.895E-12	7.746
j8gm1ac1q	52561.105	2002.782	2.937E-12	7.730
j8gm2as2q	52682.547	2003.115	3.181E-12	7.643	7.646	0.006
j8gm2as6q	52682.551	2003.115	3.198E-12	7.638
j8gm2ascq	52682.559	2003.115	3.174E-12	7.646
j8gm2asqq	52682.570	2003.115	3.148E-12	7.655
j8ma3adiq	52803.055	2003.445	3.058E-12	7.687	7.651	0.021
j8ma3admqq	52803.086	2003.445	3.194E-12	7.639
j8ma3adsq	52803.094	2003.445	3.184E-12	7.642
j8ma3ae5q	52803.156	2003.446	3.208E-12	7.634
j8ma4aqgq	52840.148	2003.547	2.178E-12	8.055	8.063	0.008
j8ma4aqq	52840.152	2003.547	2.137E-12	8.076
j8ma4aqppq	52840.156	2003.547	2.171E-12	8.058
j8ma4ar4q	52840.168	2003.547	2.159E-12	8.065
j8ma6aqgq	52957.805	2003.869	2.619E-12	7.855	7.840	0.015
j8ma6aykq	52957.809	2003.869	2.628E-12	7.851
j8ma6ayppq	52957.848	2003.869	2.710E-12	7.817
j8ma6az4q	52957.859	2003.869	2.664E-12	7.836
HRC/F330W Filter						
j8gm1aacq	52561.043	2002.782	3.306E-12	7.602	7.621	0.014
j8gm1aadq	52561.043	2002.782	3.253E-12	7.619
j8gm1aaqq	52561.051	2002.782	3.243E-12	7.623
j8gm1aarq	52561.051	2002.782	3.189E-12	7.641
j8gm1abrq	52561.098	2002.782	3.378E-12	7.578	7.608	0.021
j8gm1absq	52561.102	2002.782	3.292E-12	7.606
j8gm1ac2q	52561.105	2002.782	3.273E-12	7.612
j8gm1ac3q	52561.109	2002.782	3.201E-12	7.637
j8gm2as3q	52682.547	2003.115	3.327E-12	7.595	7.598	0.002
j8gm2as7q	52682.551	2003.115	3.312E-12	7.600
j8gm2asgq	52682.563	2003.115	3.313E-12	7.599
j8ma3adjq	52803.055	2003.445	3.913E-12	7.419	7.379	0.023

Table 3—Continued

Dataset	MJD	Year	Flux ^c	Magnitude ^a	Average ^b	σ^b
j8ma3adnq	52803.090	2003.445	4.095E-12	7.369
j8ma3adwq	52803.098	2003.445	4.112E-12	7.365
j8ma3ae9q	52803.160	2003.446	4.119E-12	7.363
j8ma4aqhq	52840.148	2003.547	3.671E-12	7.488	7.494	0.003
j8ma4aqlq	52840.152	2003.547	3.649E-12	7.495
j8ma4aqtq	52840.160	2003.547	3.648E-12	7.495
j8ma4ar8q	52840.176	2003.547	3.642E-12	7.497
j8ma6aqhq	52957.805	2003.869	4.643E-12	7.233	7.222	0.008
j8ma6aylq	52957.809	2003.869	4.695E-12	7.221
j8ma6aytq	52957.852	2003.869	4.738E-12	7.211
j8ma6az8q	52957.852	2003.869	4.678E-12	7.225
HRC/F550M Filter						
j8gm1aafq	52561.043	2002.782	3.700E-12	7.479	7.485	0.006
j8gm1aatq	52561.051	2002.782	3.663E-12	7.491
j8gm1abwq	52561.102	2002.782	3.755E-12	7.463	7.475	0.014
j8gm1ac5q	52561.109	2002.782	3.649E-12	7.494
j8gm1ac4q	52561.109	2002.782	3.745E-12	7.466
j8gm2as4q	52682.551	2003.115	4.129E-12	7.360	7.359	0.004
j8gm2as8q	52682.555	2003.115	4.162E-12	7.352
j8gm2asjq	52682.566	2003.115	4.134E-12	7.359
j8gm2asxq	52682.578	2003.115	4.118E-12	7.363
j8ma3adkq	52803.059	2003.445	4.963E-12	7.161	7.126	0.020
j8ma3adoq	52803.090	2003.445	5.156E-12	7.119
j8ma3adzq	52803.102	2003.445	5.168E-12	7.117
j8ma3aecq	52803.164	2003.446	5.206E-12	7.109
j8ma4aqiq	52840.148	2003.547	5.259E-12	7.098	7.099	0.003
j8ma4aqmq	52840.152	2003.547	5.250E-12	7.100
j8ma4aqwq	52840.164	2003.547	5.234E-12	7.103
j8ma4arbq	52840.180	2003.547	5.272E-12	7.095
j8ma6ayiq	52957.805	2003.869	6.851E-12	6.811	6.807	0.004
j8ma6aymq	52957.813	2003.869	6.907E-12	6.802
j8ma6aywq	52957.855	2003.869	6.890E-12	6.804
j8ma6azbq	52957.867	2003.869	6.849E-12	6.811

^aMagnitude on the STMAG system.

^bThe average and sigma of individual measurements in an exposure set. These values are plotted in Figure 6.

^cSTMAG flux units are $\text{erg}/\text{cm}^2/\text{s}/\text{\AA}$.